

Using a Localized Fluorescent Dye To Probe the Glass/Resin Interphase

JOSEPH L. LENHART^{1*}, JOHN H. VAN ZANTEN², JOY P. DUNKERS¹,
and RICHARD S. PARNAS³

¹*Polymers Division
National Institute of Standards and Technology
Gaithersburg, MD 20899*

²*Chemical Engineering Department
North Carolina State University
Raleigh, NC 27695*

³*Institute of Materials Science and Chemical Engineering Department
University of Connecticut
Storrs, CT 06296*

A novel technique has been developed to study the buried polymer/substrate interfacial regions by localizing a fluorescent probe on the substrate surface. Epoxy functional multi-layers of silane coupling agents were deposited on glass and doped with small amounts of a fluorescently labeled silane-coupling agent (FLSCA). When the dye-doped silane layers were immersed in an epoxy/amine cured resin, a blue shift in the emission maximum was measured after resin cure. Silane layers of varying thickness were tested. Thicker layers showed smaller fluorescence shifts during cure, suggesting incomplete resin penetration into these layers. The fluorescence sensitivity to the interfacial reaction was verified with external reflection Fourier Transform Infrared Spectroscopy (FTIR) of the silane layers immersed only in the amine hardener.

INTRODUCTION

It has been demonstrated that for many polymers, the properties near a solid surface can be different from those of the bulk polymer. The mobility of the polymer in the interfacial region is strongly dependent on the interaction between the polymer and the substrate. For thermoplastic polymers, preferential segregation of low molecular mass polymer fractions or chain ends to the interface (1) and lower entanglement density near the interface (2) will reduce the glass transition (T_g) in this region. Keddie *et al.* used ellipsometry to observe that the glass transition of thin polystyrene films on silicon oxide surfaces was lower than the bulk T_g (3). Reiter observed, using X-ray reflectometry, that thin polystyrene films could de-wet a silicon wafer even below the T_g of the bulk polymer, suggesting a lower effective T_g in the thinner films (4). The

interaction between the silicon oxide surface and polystyrene is weak. On the other hand, with hydrogen-passivated silicon wafer surfaces, significant increases in the T_g of thin polystyrene films have been observed (5).

For thermosetting resins near a solid surface, the problem is more complicated than with thermoplastic polymers. In addition to the effects of the solid surface, the thermosetting reaction occurs in the presence of the substrate. The kinetics of the interfacial reaction can be altered by the substrate surface functionality. Thermosetting resins can contain impurities, and often a mixture of many monomers, which can vary both in composition and molecular mass (6, 7). Preferential diffusion of different monomers or low molecular mass plastizers to the surface can change the interfacial cure behavior. The substrate surface is often coated with a sizing layer (often a silane coupling agent) to promote adhesion and durability at the interface (8). The presence of the sizing layer, interpenetration between the sizing layer and the curing thermoset, and potential reactivity between the sizing and resin can further alter the interfacial structure. The cure difference near the

*Corresponding author. Polymers Division; National Institute of Standards and Technology; 100 Bureau Drive Stop 8541; Gaithersburg, MD 20899-8541; jlenhart@nist.gov

EXPERIMENTAL

The measurement uncertainty given in the experimental procedure description or shown in the experimental results represents a range of values. For some of the experimental results, the uncertainty is shown as an estimated standard deviation based on measurements taken on at least five samples and multiple measurements per sample.

Unless otherwise stated, all chemicals were used as obtained from Aldrich Chemical Company (Milwaukee, WI). FLSCA was synthesized by a method described previously (9–12). Glycidoxypropyltrimethoxysilane (GPS) was used as received from Gelest (Tulleytown, PA) (16).

The resin system used in this study was an amine-hardened epoxy system (see Fig. 2). The resin system was composed of a stoichiometric mixture of diglycidyl ether of bisphenol A (DGEBA) (Tactix 123, Dow Chemical Company) and poly(propylene glycol) bis(2-amino propyl ether), (Jeffamine D230 or D400, Aldrich Chemical Company). For the amine hardener, the number average molecular mass was either (230 or 400) g/mol (D230 or D400 respectively). The two components were mixed together with a mechanical stirrer and then degassed under vacuum for 10 min prior to use. At room temperature, this resin system reacts slowly, so a negligible amount of reaction occurs during mixing and degassing. Neither the epoxy resin nor hardeners were purified.

For some experiments, either DMANS or FLSCA were dissolved into the bulk resin. For these experiments the dye concentration was adjusted so the absorption was in the linear range (17). This helped avoid inner-filter effects, which can skew the fluorescence emission at high dye concentrations.

Coupling agent layers were grafted to glass microscope cover slips (Fisher Scientific, Pittsburgh, PA)

using an ethanol-based deposition procedure as described previously (9, 17). GPS and FLSCA were added to an ethanol/water mixture with the volume fraction of ethanol equal to 95%, under slightly acidic conditions. To adjust the thickness of the silane layers, the total silane concentration in the ethanol/water mixture was varied from 0 to 0.2 mmol/mL or volume fraction of 0% to 5%. The molar ratio of FLSCA to GPS in the deposition solution ranged from 0.004 to 0.006. After hydrolysis of the coupling agents, clean glass microscope cover slips were added to the deposition solution. The coupling agents adsorb to the glass surface for 10 min. The coated cover slips were then cured at $100 \pm 2^\circ\text{C}$ for 1.5 ± 0.2 h. After curing, the cover slips were washed by two successive dips in clean ethanol for 30 ± 5 s. During the ethanol dip, the coated cover slips were vigorously shaken. The purpose of this wash was to remove excess dye and weakly adsorbed coupling agent that had deposited on the surface during solvent evaporation. The washed cover slips were dried for 1 ± 0.1 h at $100^\circ\text{C} \pm 2^\circ\text{C}$. After drying, the samples were sealed in a glass vial and stored in the dark at room temperature until fluorescence measurements were made the following day.

After the FLSCA/GPS layers were grafted to the glass cover slips, each coated cover slip was sandwiched with uncured epoxy resin between two uncoated glass cover slips (see Fig. 3). The range of the thickness of the epoxy resin in the sandwich was 25 to 100 μm . This thickness is large enough that the epoxy in the sandwich is similar to bulk resin. Excitation light was sent through the uncoated cover slip and the epoxy resin. The fluorescence was collected from the FLSCA/GPS layer, buried under the thick epoxy sandwich. The fluorescence from grafted FLSCA was measured in uncured resin and cured resin. The resin sandwich sample was cured for 4 ± 0.1 h at $100^\circ\text{C} \pm 2^\circ\text{C}$, followed by a 1 ± 0.1 h postcure at $130^\circ\text{C} \pm 5^\circ\text{C}$. For samples of

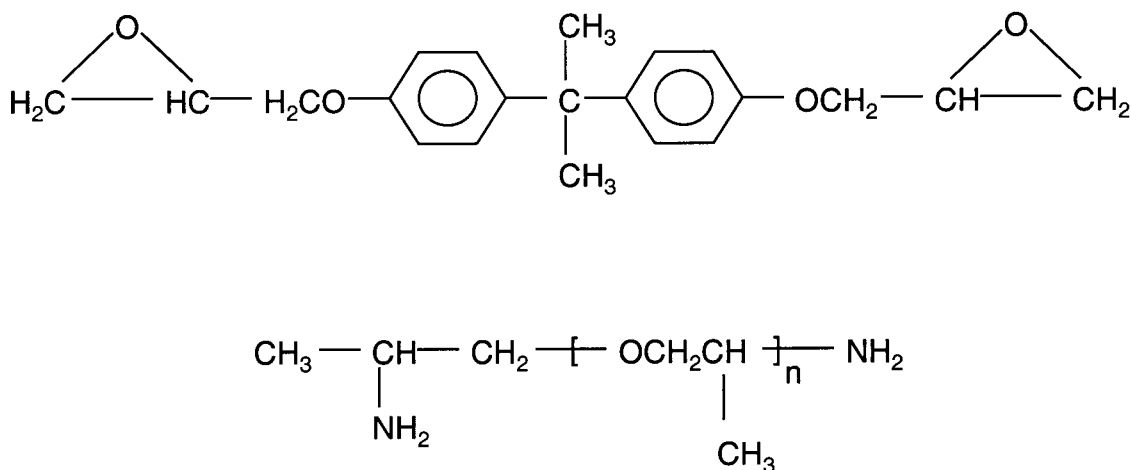


Fig. 2. The amine hardened epoxy resin system is shown above. The top structure is the DGEBA monomer. The bottom structure is the diamine hardener. The "n" can be adjusted so that the number average molecular mass of the hardener is either 230 g/mole or 400 g/mole.

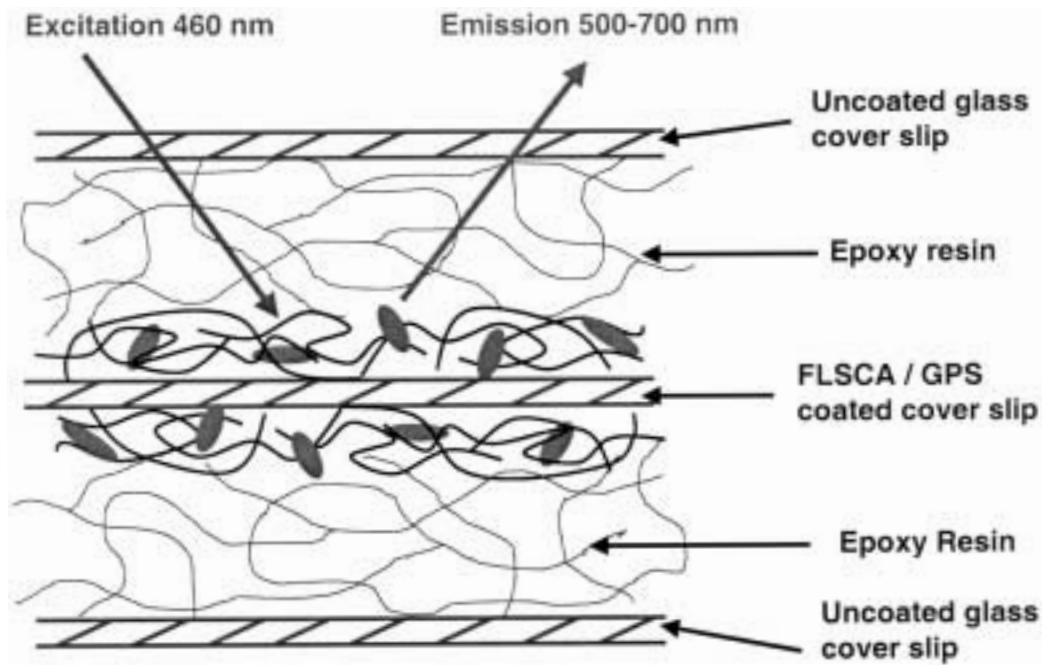


Fig. 3. A FLSCA/GPS coated glass microscope cover slip was sandwiched between epoxy resin and two uncoated cover slips. The fluorescence was measured before and after resin cure by sending light through the sandwich sample and collecting the emission at an offset angle.

DMANS or FLSCA in bulk epoxy, the center cover slip in the sandwich was not coated with a FLSCA/GPS coupling agent layer, but the dye was dissolved into the epoxy resin used in the sandwich structure.

Scanning electron microscopy (SEM) was used to measure the thickness of the silane coupling agent layers. After the coupling agents were deposited onto the glass surface, the glass surface was scored with a diamond-tip razor. The sample was snapped and mounted vertically onto the SEM mount. Carbon paint was used to mount the glass sample. After the carbon paint dried, the sample was coated with gold. SEM measurements were made on the un-scored side of the cross-sectioned sample with a Hitachi S4500 Field Emission SEM (Nissei Sangyo Co., Rolling Meadows, IL) using a working distance of 7 mm, and an accelerating voltage of 7 kV. The detector was the upper secondary electron detector.

External reflection FTIR experiments were conducted on the silane coupling agent layers grafted to the glass surface using a 60° angle of incidence on a Nicolet Magna 550 FTIR (Madison, WI) using 1200 scans at a resolution of 4 cm⁻¹ and a mercury-cadmium-telluride detector. The FTIR experiment is not an attenuated total internal reflection (ATR) technique. The IR radiation passes through the air and into the FLSCA/GPS sample. The IR radiation passes twice through the sample thickness. The purpose of the 60° angle of incidence is to increase the path length through the sample.

RESULTS AND DISCUSSION

In Fig. 4, typical fluorescence emission spectra from the grafted FLSCA/GPS sandwich structures before and after resin cure are shown. When the layer is immersed in uncured DGEBA/D230, the emission maximum, λ_{\max} , occurs at 637 ± 3 nm. In cured resin, λ_{\max} is blue shifted and occurs at 599 ± 2 nm. The fluorescence intensity also increases during resin cure. The layer thickness for data shown in Fig. 4 was 0.52 ± 0.27 μm, as measured by SEM. The large value in the standard deviation indicates the non-uniformity of the layer thickness (rather than instrumental uncertainty). Further, while this standard deviation was calculated from 10 scans on four different samples, significant thickness variations also exist on a particular sample. The uncertainty in the emission maximum is a standard deviation from multiple measurements on at least 5 samples. The relative standard uncertainty in the fluorescence intensity is 15%.

Both the intensity change and the emission shift can potentially be correlated with the extent of the epoxy cure. Because no internal standard is present to normalize the intensity, we will only discuss the shift in the emission maximum. Shifts in the emission spectrum of fluorescent dyes can be correlated with the extent of resin cure (18–25). The blue shift and intensity increase from DMANS during resin cure is due to the epoxy cure reaction. As the resin reacts, the dielectric constant that is observed by the excited dye

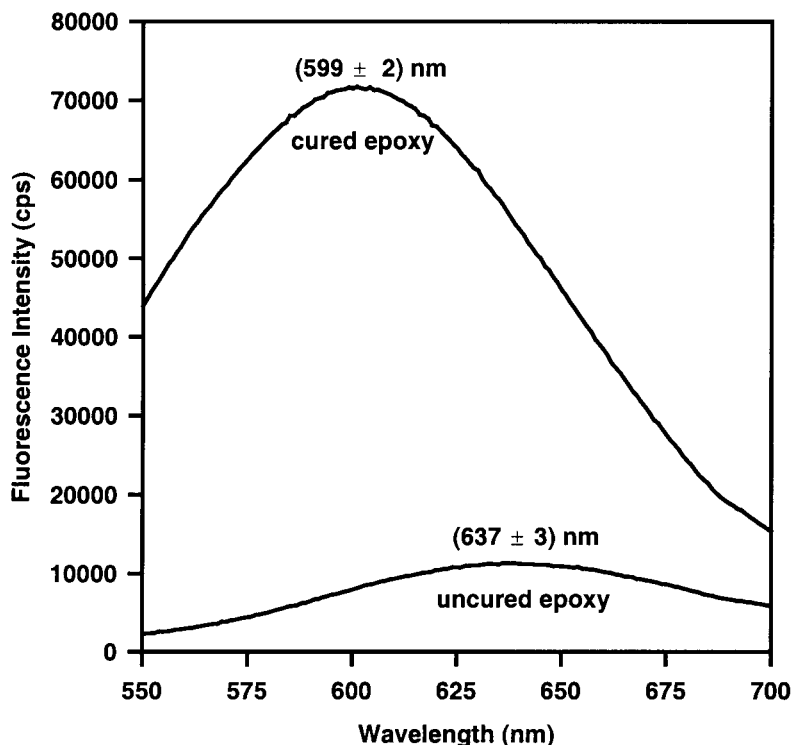


Fig. 4. A blue shift in the emission maximum, and an increase in the fluorescence intensity could be followed from grafted FLSCA in the sandwich sample during resin cure. Since no internal standard was present to normalize the intensity it is more practical to monitor the wavelength shift.

decreases. In addition, the refractive index increases due to resin densification. Although these factors have been discussed in detail elsewhere (9, 17), they will be briefly discussed here to aid the data interpretation. The Lippert Equation (Eq 1) describes how the solvent influences the position of the fluorescence emission (26).

$$\nu_a - \nu_f \cong \frac{2}{hc} \left(\frac{\epsilon - 1}{2\epsilon + 1} - \frac{n^2 - 1}{2n^2 + 1} \right) \frac{(\Delta\mu)^2}{a^3} + \text{const} \quad (1)$$

Here ϵ is the solvent dielectric constant, n is the refractive index of the solvent, c is the speed of light, h is Planck's constant, a^3 is the volume occupied by the fluorophore, $\Delta\mu$ is the dipole moment change of the fluorophore between the ground and excited state, and ν_a and ν_f are the wave numbers (cm^{-1}) of the absorption and emission intensity maximum, respectively. The Stoke's shift is defined as the difference between the absorption and emission intensity maxima of the fluorophore. It is a measure of the energy dissipated from the excited state molecule before releasing a fluorescence photon. The refractive index contribution accounts for the ability of the solvent electrons to reorient in order to stabilize the dipole moment of the fluorophore. The dielectric constant term accounts for the solvent relaxation process, which will decrease the energy difference between the ground and excited states. The constant term in Eq 1 accounts for additional mechanisms of energy dissipation, such as vibrational relaxation.

In Eq 1, the important terms involving the polymer environment (surrounding grafted FLSCA) are the dielectric constant and the refractive index. The local

dielectric constant that is observed by the fluorescent dye decreases during resin cure. This decrease can be caused by a decrease in the dielectric mobility, and/or a decrease in the dipole strength of the molecules. The dielectric mobility slows owing to the increasing molecular mass and cross-link density of the epoxy during cure. The dipole moments of the molecules can also potentially change because of the epoxy/amine reaction. From Eq 1, a decrease in the observed dielectric constant will cause the fluorescence emission to occur at shorter wavelengths. As the resin cures, the refractive index increases due to the increase in polymer density. Also from Eq 1, an increase in the refractive index will also contribute to the blue shift in emission during cure.

In Fig. 5 the total fluorescence shift (blue shift of the peak maximum during resin cure) from grafted FLSCA/GPS layers (of varying thickness) immersed in DGEBA/D230 or DGEBA/D400 is shown. The initial starting point for the FLSCA/GPS layers in uncured resin is similar for each layer thickness. After resin cure, however, the magnitude of the fluorescence shift is dependent on the layer thickness. Thicker layers showed smaller blue shifts. As a control, the fluorescence of FLSCA in bulk resin was recorded and is also shown in Fig. 5. The shift for FLSCA dissolved in bulk resin was larger than from FLSCA/GPS layers grafted to the glass surface. The fluorescence maximum for FLSCA in bulk uncured resin ranged from 627 to 632 nm. This maximum is slightly different than the fluorescence of the FLSCA/GPS layers in uncured resin which ranged from 634 to 638 nm. This difference indicates that the bulk uncured resin has slightly different dielectric and

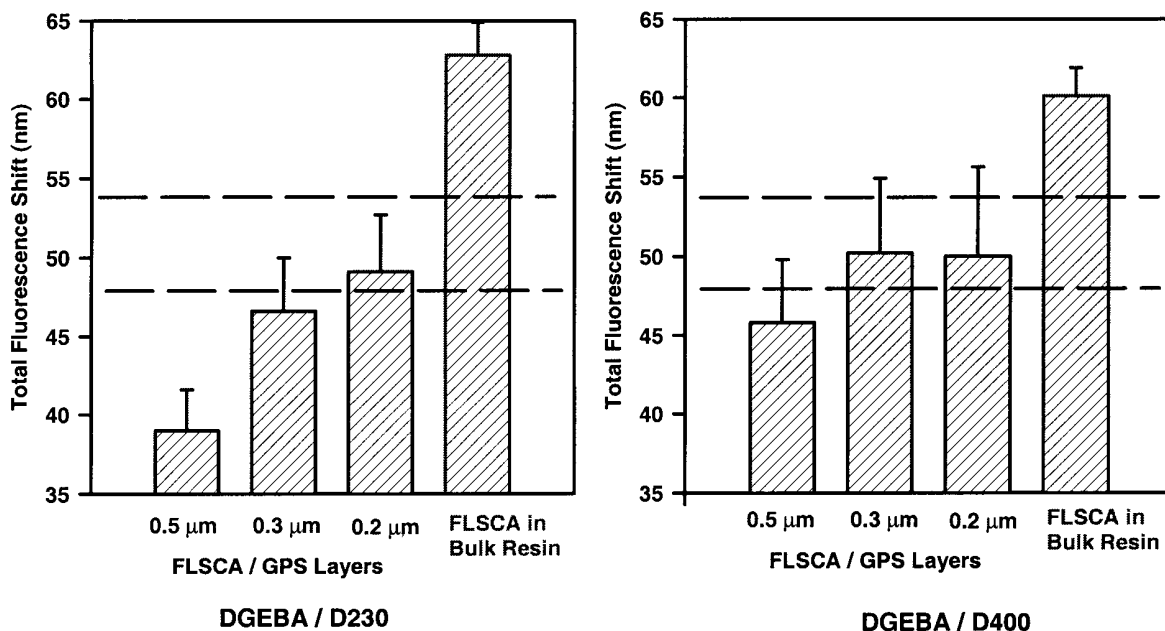


Fig. 5. The magnitude of the fluorescence shift during cure was dependent on the thickness of the silane layer. Thicker layers showed smaller shifts, suggesting incomplete penetration of the resin monomers into the thickest layers. The uncertainty in the fluorescence shift is a standard deviation from measurements on at least 5 samples and multiple measurements per sample. The standard deviation of the silane thickness was approximately 50% of the average thickness value.

refractive index properties compared to the FLSCA/GPS layer. However, the difference is small, suggesting that the chemical reaction between the epoxy and the amine is the primary cause of the fluorescence shift during cure, rather than simply penetration of the resin monomers into the FLSCA/GPS layers.

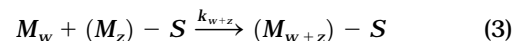
The fluorescence shift from FLSCA/GPS grafted layers during resin cure is an indication that the resin molecules are able to penetrate the silane layer. If no interpenetration occurs, then the local environment surrounding the dye molecules would not change during cure and no shift would be observed. A difference in the fluorescence shift during resin cure suggests a difference in chemical composition. The larger shift, from thinner FLSCA/GPS layers, indicates increased interpenetration between the silane layer and resin. From the data in Fig. 5, the interfacial composition appears to be determined in part by the competition between monomer diffusion into the sizing layer and the resin reaction kinetics. An interesting consequence of this competition is that a smaller decrease in the fluorescence shift occurs in the DGEBA/D400 compared to the DGEBA/D230, as the layer thickness increased. The DGEBA/D400 resin takes longer to gel than the DGEBA/D230 (30 min vs. 15 min at 100°C), allowing more time for resin penetration into the thicker layers. We propose that resin gelation occurs before complete penetration into the thickest layers, especially in the case of the DGEBA/D230.

The epoxy/amine polymerization process can be modeled by a general condensation reaction scheme with three steps: a) homopolymerization of the resin monomers (Eq 2); b) graft polymerization where the

resin monomers attach to the grafted silane layer (Eq 3); and c) condensation of grafted polymer chains (Eq 4).



where M_x and M_y are partially cured networks of amine and epoxy polymers. Sections of the partially cured network can also react with the silane layer on the glass surface in the graft polymerization step:



where $(M_z) - S$ indicates a surface attached group on the glass surface. Two grafted chains can also condense with one another:



Where $S - (M_a)$ is a grafted chain with an amine end group and $S - (M_e)$ is a grafted chain with an epoxy end group.

While this model is complicated, it can be simplified by neglecting the etherification reaction. In addition, we can assume that reactions within the silane layer primarily involve monomers or very low molecular weight chains. This assumption is reasonable because the GPS layer must swell to accommodate the reacting network chains. Because (χn) is large for the large molecular weight chains, it is thermodynamically unfavorable for these larger network chains to penetrate the GPS coating. This means that the subscripts (x , y , and w) in the above equations are around 1 or 2 but not 10 or 100. Given these assumptions we write a simplified mass balance on the resin monomers in the silane layer:

$$\frac{\partial C_m}{\partial t} = D_m \left(\frac{\partial^2 C_m}{\partial Z^2} \right) - [k_h f_h(C_m) + k_g f_g(C_m)] \quad (5)$$

where C_m is the concentration of the monomer (either amine or epoxy) in the silane layer, D_m is the diffusion constant for the resin monomer in the silane layer, k_h and k_g are the rate constants for the homopolymerization (Eq 2) and graft polymerization (Eq 3) respectively, and $f_h(C_m)$ and $f_g(C_m)$ are the kinetic models for the homopolymerization and graft polymerization respectively. In this model we assume that the silane layer does not diffuse away from the glass surface, which is a reasonable assumption considering that the layers were washed after deposition.

After gelation, the diffusion constant drops dramatically and we replace D_m in Eq 5 with D_{gel} , representing the slow diffusion of resin monomers after gelation. This mass balance can be non-dimensionalized:

$$\frac{\partial \theta_m}{\partial \tau} = \frac{D_m}{k_h L^2} \left(\frac{\partial^2 \theta_m}{\partial Z^2} \right) - \left[f_h(\theta_m) + \frac{k_g}{k_h} f_g(\theta_m) \right] \quad \text{for } \tau < k_h t_{gel} \quad (7)$$

$$\frac{\partial \theta_m}{\partial \tau} = \frac{D_{gel}}{k_h L^2} \left(\frac{\partial^2 \theta_m}{\partial Z^2} \right) - \left[f_h(\theta_m) + \frac{k_g}{k_h} f_g(\theta_m) \right] \quad \text{for } \tau > k_h t_{gel} \quad (8)$$

θ_m is dimensionless concentration, τ is dimensionless time, Z is dimensionless position, L is the silane layer thickness, t_{gel} is the gel time of the resin. For $t \ll t_{gel}$ we compare L^2/D_m with $1/k_h$ to determine if the interfacial development is limited by the reaction or diffusion process. For $t > t_{gel}$ diffusion essentially stops and the reaction proceeds slowly to completion. Since D_m is much larger than D_{gel} , the interfacial composition profile is essentially "frozen" in place once resin gelation occurs.

Using the gel times for the two resin systems (15 min at 100°C for DGEBA/D230 and 30 min at 100°C for DGEBA/D400) we can estimate the diffusion constant for the resin monomers within the silane layer by $D \sim L^2/t_{gel}$. For the DGEBA/D230 system, the transition from "complete" to "incomplete" penetration occurs between the 500-nm-thick and 300-nm-thick layers. A similar transition range was observed for the DGEBA/D400 system although much less dramatic than for the D230 system. Using this thickness range, the estimated diffusion constant will range from 10^{-12} to 10^{-13} cm²/s. This agrees well for diffusion measurements of small molecule probes in rubbery polymer films (27).

Fluorescence can be correlated with the extent of resin cure (18–25), but it is an indirect measure of the cure reaction. Therefore, performing external measurements on model samples is important for calibrating the fluorescence response. We propose that the blue shift during resin cure is due to the reaction between the epoxy and amine functional groups in the

interfacial region. Infrared measurements on the buried interfacial region are difficult, however, owing to the similar functionality of the GPS coating and the DGEBA monomer. In order to relate the fluorescence response of grafted FLSCA to the interfacial cure reaction, control experiments were performed on a model system. In the first of these control experiments, a 0.52 ± 0.27 - μm -thick layer was immersed in the D230 hardener only. The fluorescence was measured at time zero, and after 20 h of immersion in the hardener at 100°C. After 20 h in the hardener a fluorescence shift of 49 ± 2 nm was observed. A similar thickness layer was immersed in the primary mono-amine, n-propylamine. After 20 h at 100°C in n-propylamine, a fluorescence shift of 51 ± 2 nm was observed. The range of the fluorescence shift for these control experiments is shown in Fig. 5 by the horizontal dashed lines. The uncertainty in the fluorescence shift is a standard deviation from multiple measurements on at least 5 samples.

These control experiments were vital for two reasons. First, the reaction between the epoxide on GPS and the amine on the hardener was shown to be a major factor contributing to the fluorescence shift. Although when FLSCA/GPS layers are immersed in a mixture of epoxy and hardener, the fluorescence response may not distinguish a reaction between the hardener and GPS from a reaction between hardener and epoxy monomers that have diffused into the silane layer. Second, they gave an indication of the maximum fluorescence shift that is expected without the complications due to resin gelation, which dramatically slows the diffusion. An additional control experiment was to immerse a FLSCA/GPS layer in just DGEBA. In that case the fluorescence shift was small, ranging from 5 to 7 nm towards shorter wavelengths. DGEBA most likely penetrates into the FLSCA/GPS layer, but the large shift does not occur unless amine hardener is present to react with the epoxy groups on GPS or with DGEBA monomers that have diffused into the silane layer. The emission maximum for FLSCA in the DGEBA monomer was 626 nm. Because the FLSCA/GPS layers had a maximum near 638 nm when not immersed in resin, the diffusion of DGEBA into the layer should cause only a small blue shift in emission, due to the slightly less polar nature of the DGEBA monomer. The emission of FLSCA in the bulk hardeners occurs at 629 and 639 nm, respectively, for the D400 and D230 Jeffamines. Diffusion of the hardener into the layer without chemical reaction between the hardener and GPS would cause little or no fluorescence shift due to the similar emission spectra of FLSCA in the GPS layer and FLSCA in the pure hardener. So the fluorescence shift can be used to study interpenetration of monomers into the silane layer. However, the fluorescence shift is actually caused by the chemical reaction between the amine and epoxy functional groups. Increased interpenetration leads to an increase in the extent of this interfacial reaction, and a larger fluorescence shift.

To verify that the epoxy groups on the GPS layer have reacted with the amine on the hardener, external reflection FTIR experiments were conducted on the FLSCA/GPS layer before and after 20 h immersion in the hardener. The FTIR spectra are shown in Fig. 6. The bottom curve is for the FLSCA/GPS layer before immersion in the hardener. The broad band near 3500 cm^{-1} is due to the Si-OH absorbance (28). The peaks at 3050 and 3000 cm^{-1} are due to the CH and CH_2 stretching modes, strained in the epoxide ring in GPS (28). The top spectrum is for the layer after immersion in the hardener. The two peaks at 3050 and 3000 cm^{-1} have decreased dramatically, indicating that the epoxy rings on the GPS have opened. A large broad absorbance also occurs near 3450 cm^{-1} . This band may be due to the NH stretching of the amine (28) on incompletely reacted hardener molecules that have penetrated into the silane layer, or the peak may also be due to the hydroxyl groups that have formed from the epoxy ring on GPS during the GPS/amine reaction. A clear shoulder also appears in the amine peak near 3520 cm^{-1} , further indicating the presence of hydroxyls. The residual hydroxyls could be a consequence of the epoxy/amine reaction or incomplete condensation of the silanol groups in the silane layer. The peak that appears near 2975 cm^{-1} is likely due to the stretching vibrations of the CH groups that were on the epoxy ring. Once the epoxy ring opens, these vibrations are not strained and will occur at lower energies.

Figure 6 verifies that the hardener was able to penetrate into the silane layer. After the layer was immersed in D230, the surface was rinsed with clean acetone to remove the excess hardener before the FTIR spectrum was collected. The amine absorption must have been due to hardener molecules that have diffused into the FLSCA/GPS layer. The disappearance of the strained CH stretching modes suggests a reaction between the amine on the hardener and the epoxide on GPS. The corresponding fluorescence shift after immersion of the FLSCA/GPS layer in the hardener indirectly relates the fluorescence shift to this reaction.

The FTIR spectra relate the fluorescence shift to the epoxy/amine chemical reaction in the silane layer. However, because of the inaccurate baseline for the FLSCA/GPS layer in the hardener, it is difficult to determine if the strained CH stretching vibrations have completely disappeared. For example, inaccessible epoxy groups on GPS may exist in the layer even with equilibrium hardener penetration into the layer. However, because diffusion of D230 into the layer was not hindered as a result of resin gelation, we propose that 48 to 54 nm is the total fluorescence shift that is expected from a FLSCA/GPS layer that is completely penetrated by the resin monomers. This range is shown in Fig. 5 by the dotted lines. The fluorescence shift during cure approaches this range in thinner layers.

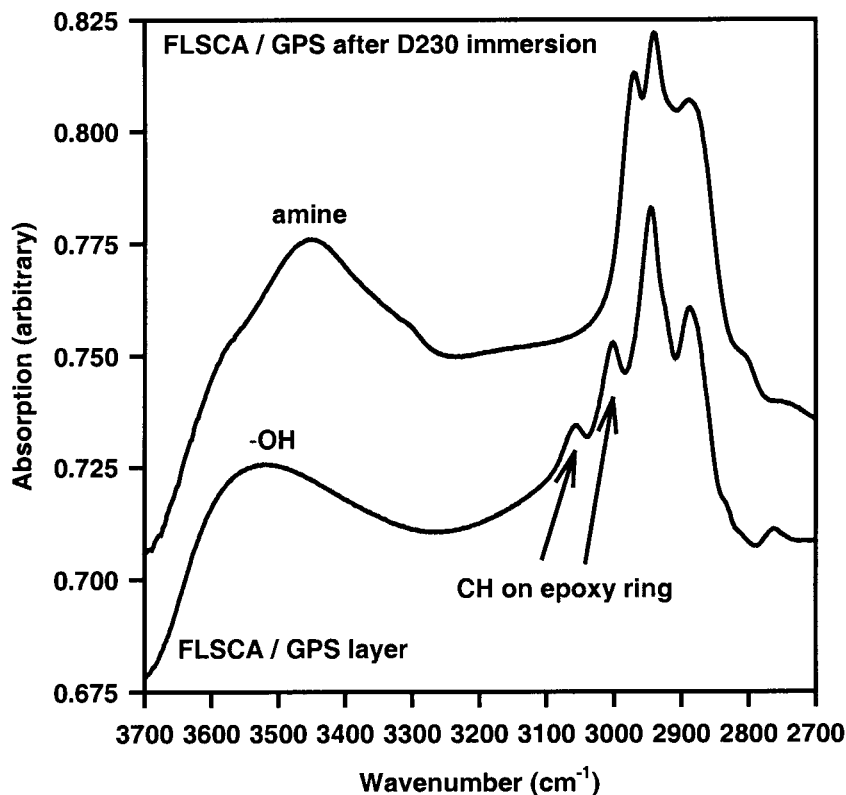


Fig. 6. Penetration of the hardener into the FLSCA/GPS layers was verified with front reflection FTIR. The disappearance of the strained CH stretching modes of the epoxide suggests reaction between the hardener and the GPS.

It is interesting to note that the total shift for FLSCA in bulk epoxy resin ranged from 60 to 65 nm after complete resin cure in a stoichiometric mixture. The maximum shift from the FLSCA/GPS layers was approximately 50 to 55 nm. Several possible scenarios could explain this difference. First, unreacted epoxy groups may remain within the FLSCA/GPS layer. In order for the resin monomers to penetrate the GPS coating, the layer must swell. Depending on the degree of GPS condensation, some of the epoxy groups may remain inaccessible. In addition, because the layer must swell to accommodate the resin monomers, complete equilibrium penetration of the layer by the resin could still lead to off-stoichiometric cure in the interfacial region, and a smaller fluorescence shift. Owing to the inaccuracy in determining a baseline, estimating the amount of inaccessible or unreacted epoxy groups from the FTIR data in Fig. 6 is difficult.

The smaller fluorescence shift from the thin FLSCA/GPS layers compared with the dye in bulk resin could also be due to the extent of the amine reaction. When the amine hardener penetrates the layer and reacts with an epoxide on GPS, the monomer becomes immobile. The surrounding GPS molecules are also immobile, because of attachment within the silane structure. It is possible that the amine is left as a secondary amine rather than being completely converted to a tertiary amine by reaction with another epoxy. On the other hand, in the bulk resin the secondary amines can still find another epoxy (particularly before the diffusion limited regime after gelation). A final possibility is that the epoxy groups on GPS have opened but did not react with hardener molecules. This would lead to an excess of polar hydroxyl groups in the interfacial region.

These scenarios all suggest that the interfacial region is more polar than the bulk resin, which could have an important impact on the adhesive strength and durability of the epoxy/glass bond. For example, water adsorption might be expected to be more prominent in the more polar interfacial region.

CONCLUSION

Epoxy functional silane coupling agent multi-layers on glass surfaces were doped with small amounts of a fluorescent-labeled silane coupling agent (FLSCA). When the coupling agent layers were immersed in an amine cured epoxy resin, a blue shift in the emission maximum from grafted FLSCA could be followed during resin cure. By immersing the silane layers in just hardener or a mono-functional amine, the fluorescence shift was shown to be a consequence of the chemical reaction between the epoxy group in the silane layer and the amine group in the hardener. This mechanism was verified by external reflection FTIR on the same sample. The magnitude of the fluorescence shift was dependant on the thickness of the silane coupling agent layer. Thicker layers showed smaller fluorescence shift, suggesting a lower interfacial extent of reaction, and an inability of the resin to completely penetrate thicker

silane coatings. These results show that the interfacial region can be dictated by the competition between resin diffusion into a sizing layer on the substrate surface and the polymer reaction kinetics, which will slow the diffusion process. The technique provides a novel way to study the interfacial chemical composition and interpenetration between the resin monomers and a sizing layer on the substrate surface.

REFERENCES

1. A. M. Mayes, *Macromolecules*, **27**, 3114 (1994).
2. H. R. Brown and T. P. Russell, *Macromolecules*, **29**, 798 (1996).
3. J. L. Keddie, R. A. L. Jones, and R. A. Cory, *Europhys. Lett.*, **27**, 59 (1994).
4. G. Reiter, *Macromolecules*, **27**, 3046 (1994).
5. W. E. Wallace, J. H. van Zanten, and W.-L. Wu, *Phys. Rev. E*, **52**, R3329 (1995).
6. L. T. Drzal, "The Interphase in Epoxy Composites," in *Advances in Polymer Science*, p. 1, K. Dusek, ed., Springer-Verlag, Berlin (1986).
7. C. E. M. Morris, P. J. Pearce, and R. G. Davidson, *J. Adhes.*, **15**, 1 (1982).
8. E. P. Plueddemann, *Composite Materials; Volume 6: Interfaces in Polymer Matrix Composites*, Academic Press, New York (1974).
9. J. L. Lenhart, J. H. van Zanten, J. P. Dunkers, C. G. Zimba, C. A. James, S. K. Pollack, and R. S. Parnas, *J. Coll. Interface Sci.*, **221**, 75 (2000).
10. D. R. Robello, *J. Polym. Sci. Part A: Polym. Chem.*, **28**, 1 (1990).
11. F. Chaput, D. Riehl, Y. Lévy, and J.-P. Boilot, *Chem. Mater.*, **5**, 589 (1993).
12. F. Chaput, D. Riehl, J.-P. Boilot, K. Cargnelli, Canva, Y. Lévy, and A. Brun, *Chem. Mater.*, **8**, 312 (1996).
13. E. P. Plueddemann, *Silane Coupling Agents*, Plenum Press, New York (1982).
14. J. L. Lenhart, J. H. van Zanten, J. P. Dunkers, and R. S. Parnas, *SPE ANTEC*, **46**, 827 (2000).
15. W.-L. Wu, W. J. Orts, C. J. Majkrzak, and D. L. Hunston, *Polym. Eng. Sci.*, **35**, 1000 (1995).
16. Identification of any commercial products is made only to facilitate experimental reproducibility and describe experimental procedure. It does not imply endorsement by NIST or imply that the particular product is necessarily the best for the experiment.
17. J. L. Lenhart, J. H. van Zanten, J. P. Dunkers, and R. S. Parnas, *Langmuir*, **16**, 8145 (2000).
18. C. S. P. Sung and H. L. Sun, *Macromolecules*, **19**, 2922 (1986).
19. C. S. P. Sung and J. C. Song, *Macromolecules*, **26**, 4818 (1993).
20. R. O. Loutfy, *J. Poly. Sci. Part B: Polym. Phys.*, **20**, 825 (1992).
21. O. Pekcan, Y. Yilmaz, and O. Okay, *Polymer*, **38**, 1693 (1997).
22. K. F. Lin and F. W. Wang, *Polymer*, **35**, 687 (1994).
23. D. L. Woerdeman, J. K. Spoeerle, K. M. Flynn, and R. S. Parnas, *Polym. Compos.*, **18**, 133 (1997).
24. K. Hakala, R. Vatanparast, S. Li, C. Peinado, P. Bosch, F. Catalina, and H. Lemmetyinen, *Macromolecules*, **33**, 5954 (2000).
25. J.-W. Yu and C. S. P. Sung, *J. Appl. Polym. Sci.*, **63**, 1769 (1997).
26. J. R. Lakowicz, *Principles of Fluorescence Spectroscopy*, Plenum Press, New York (1983).
27. D. D. Deppe, R. D. Miller, and J. M. Torkelson, *J. Polym. Sci. B.*, **34**, 2987 (1996).
28. N. B. Colthup, L. H. Daly, and S. E. Wiberley, *Introduction to Infrared and Raman Spectroscopy*, Academic Press Inc., San Diego, Calif. (1990).